Ingrid Zaiser (Autor)

Helium and Hydrogen Isotope Adsorption and Separation in Metal-Organic Frameworks

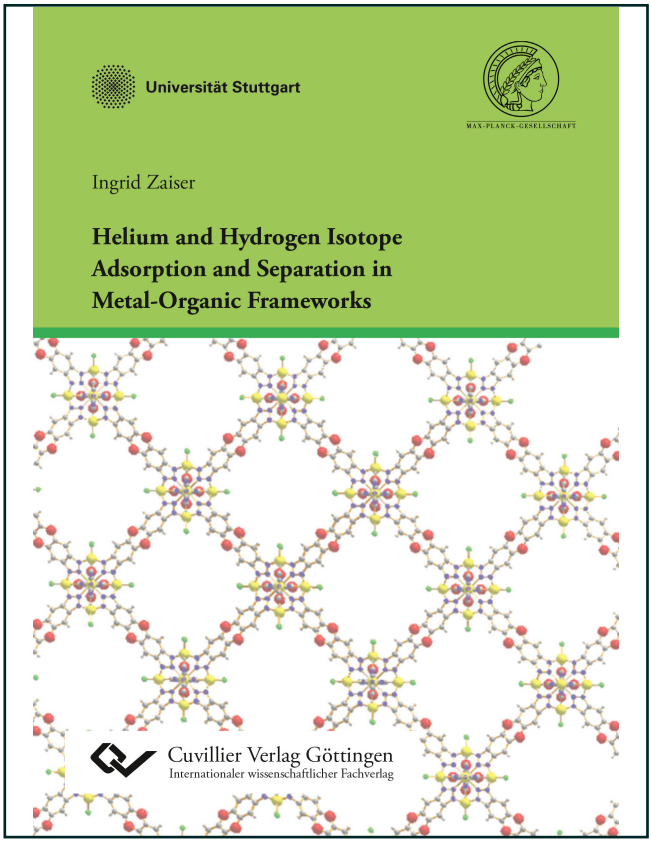

https://cuvillier.de/de/shop/publications/7372

1 Introduction

Hydrogen and helium are both lightest and most abundant elements in the universe. Still, the extraction of their rare, but highly demanded isotopes like deuterium and helium-3 is a challenging task. Deuterium occurs naturally in a low abundance of only 0.015% [1] and helium-3 is extremely rare on earth with a natural abundance of 0.00013% [2]. Many industrial and scientific applications require deuterium and cannot at all be performed with a mixture of hydrogen isotopes. Deuterium is needed for example in research reactors as a cold source, in neutron scattering and for isotopic tracing during chemical reactions. Helium-3 on the other hand is highly requested for use in neutron detectors [3] or in dilution refrigerators [4, 5] to reach extremely low temperatures of millidegrees Kelvin. Even the possibility of lunar mining [6, 7] has been taken into consideration to satisfy the demand of this precious isotope. Deuterium and helium-3 can be used as fuel for nuclear fusion. Operating with deuterium-tritium fuel for fusion is useful for studies, but less practical for commercial application. This reaction produces large amounts of radiation in form of neutrons and a substitution of the radioactive tritium with helium-3 reduces the neutron production. Recently, a breakthrough has been reported in the design of the stellarator concept Wendelstein-7X. [8] The chance of realizing nuclear fusion as future energy supply supports the great importance to extract these isotopes from their most common isotope form, i.e. hydrogen and helium-4.

A widespread technique for the extraction of molecules from gas mixtures uses shape selective microporous materials, called molecular sieves. This technique is not applicable for isotopes, as different isotopes of the same element have identical size. Nowadays deuterium is extracted via cryogenic distillation at 24 K or the Girdler-sulfide process. Both methods have very low separation factors (1.5 and 2.3, respectively [9]) and consume high amounts of energy. The standard way to produce helium-3 is coupled with the production of tritium in the nuclear weapon industry. Helium-3 is skimmed as a byproduct of the radioactive tritium decay. Direct recovery due to the occurrence of traces of helium-3 in the atmosphere and in some natural gas sources is also possible.

The high energy consumption and low efficiency of conventional isotope separation methods, which are based on mass differences, motivates to search for alternatives. Quantum Sieving has been proposed by Beenakker *et al.* [10] as a promising technique for the separation of light isotopes, which are selectively adsorbed in very small pores at low temperatures. The idea is based on the favorable adsorption of the heavier isotope with the lower zero-point energy. This isotope is preferred to enter the pores. Another concept for the separation of isotopes, called Chemical Affinity Sieving uses as well the difference in zero-point energy. [11] When the isotopes interact with strongly attractive adsorption centers, this difference can be enhanced and results in higher adsorption enthalpy of the heavier isotope and, therefore, separation.

The new class of crystalline porous materials, called metal-organic frameworks (MOFs) provides excellent candidates for the separation of isotopes by either Quantum Sieving or Chemical Affinity Sieving. MOFs are assembled by metal-ions as framework nodes which are connected via organic ligands as linkers. The great variety of the building units leads to different pore sizes and possible functionality. For Quantum Sieving, MOFs with suitable pore sizes are demanded and for Chemical Affinity Sieving, strong adsorption sites like open metal sites are required.

The separation of light isotopes is currently a topic of high interest in the scientific community. Recently, the group of the Nobel Prize holder Prof. Geim has published the separation of hydrogen isotopes with graphene and boron nitride sieves at room-temperature. [12] The greater zero-point energy of protons allows them to overcome the materials energy barriers easier. Therefore, deuterons permeate through this crystal much slower than protons, which results in a separation factor of approximately 10. This is a great result at room temperature, but from a practical point of view a preference of the less abundant deuteron over the proton would be better. In the reported case a lot of energy is spent to transport the much larger amount of protons across the sieve. Also helium isotope separation with graphene is currently investigated. Theoreticians proposed the separation of helium isotopes with nanoporous functionalized graphene membranes. [13, 14] They removed two neighbored rings of carbon in the graphene membranes and saturated the carbon atoms with hydrogen and nitrogen atoms in order to create a suitable barrier height, which leads to a higher transmission probability for helium-3. A helium-3/helium-4 ratio of 19 has been calculated for gas at 10 K, which decreases very fast to a ratio of 2 at 20 K. For testing this concept experimentally, the creation of suitable nanosized holes in graphene is still demanded.

The separation of hydrogen and helium isotopes in MOFs has been experimentally investigated with thermal desorption spectroscopy (TDS) in the present work. TDS gives a fingerprint of the adsorbed isotopes in the sample. After the material has been exposed to equimolar isotope mixtures the separation factor, called selectivity, can be directly determined from TDS spectra. The adsorbed amount of gas is proportional to the area enclosed by the TDS maxima.
Several MOFs with pore apertures meeting the size requirement for separation of hydrogen and helium isotopes with Quantum Sieving have been chosen. Adequate candidates have been found in the IFP [15–17] and MFU-4 [18] MOF series. MOFs with open metal sites are used in this work for the investigation of Chemical Affinity Sieving. One material with a very strong open copper site, named Cu(I)-MFU-4*l* [19] and three open nickel site materials, CPO-27 [20,21], DUT-9 [22] and CFA-6 [23] have been investigated.

2 Fundamentals

2.1 Adsorption in porous materials

Adsorption occurs when particles of a gas or a liquid stick to the surface of a solid material (adsorbent). In contrast to the bulk atoms of a solid, the atoms on the surface are not wholly surrounded by other atoms and therefore the bonds on the surface are unsaturated. In order to reach an energetically more favorable state the surface atoms attract the gas molecule which looses through adsorption at least one degree of freedom of translation and thus the entropy (ΔS) decreases. For any spontaneous process the Gibbs free energy decreases ($\Delta G < 0$). In accordance with the thermodynamic equation

$$\Delta G = \Delta H - T\Delta S \tag{2.1}$$

the enthalpy ΔH also decreases. The nature of the involved forces between the adsorbent and the gas molecules are of two main kinds, physical and chemical. Sharing or transfer of electrons between adsorbent and gas molecules leads to chemisorption of the gas molecule, which can dissociate on the surface. In case of chemisorption only a monolayer can be adsorbed on the surface. The chemisorption bond has the characteristics of a chemical bond and is site specific i.e. localized at active centres on the adsorbent.
The physical interaction (physisorbtion), is an exothermic process and leads to a reversible bound mono- or multilayer of gas molecules. [24] Adsorption through physisorption arises from van der Waals forces. Fluctuations in the charge distribution of polarizable molecules induces a temporary dipole, which affects the surrounding molecules by inducing a corresponding electrical moment in a near neighbor molecule leading to attractive interactions (London-type dispersion). The counterpart is the short-range repulsive interaction arising from electron orbital overlap (Pauli exclusion principle). Both forces get balanced when adsorption occurs. The Lennard-Jones potential describes the interaction between a gas molecule and an adsorbent surface in dependence of their distance r [25]:

$$V_{LJ} = 4\epsilon \left[\left(\frac{\sigma}{r}\right)^{12} - \left(\frac{\sigma}{r}\right)^{6} \right] \tag{2.2}$$

ϵ is the depth of the potential well. σ is known as the van der Waals radius and represents the smallest distance between two non-bonding particles. The r^{-6} term of the Lennard-Jones potential describes the attractive long-range interactions and has been first proposed by F. London [26] in 1930. The repulsive part has a r^{-12} dependence and is in contrast to the London dispersion interaction not theoretically justified. The Pauli repulsion is well approximated by this dependence and is quiet convenient for calculations, since it is the square of the attractive term. This potential is also valid for the adsorption of single particles on a flat surface. Figure 2.1a shows the Lennard-Jones potential including the relevant parameters.

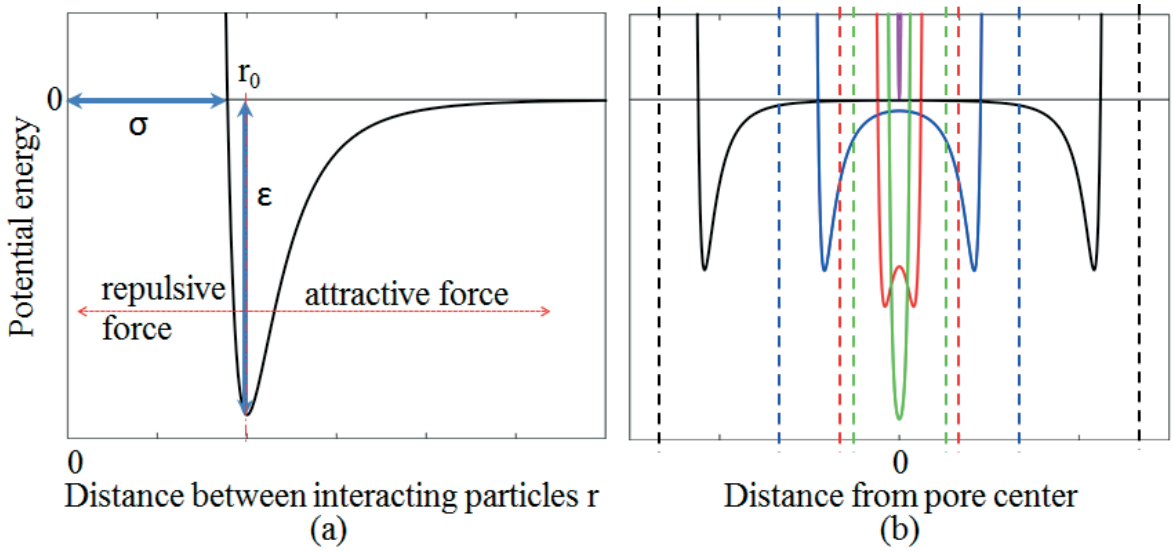

Figure 2.1: a) Lennard-Jones potential for a particle approaching a surface b) Interaction potential for a particle in slit-pores with different distances, indicated by different colors. Ratio between pore and particle diameter: 10, 5, 2.5, 2, 1. The dashed line represents the pore wall.

The adsorption in porous materials can be described in the simplest model by two flat surfaces interacting on the particle, the so-called slit pore. [27] Figure 2.1b depicts the potential of the particle in the slit pore as a function of the distance between the two surfaces for different ratios of pore and particle diameter. Compared to a single flat surface, the potential energy exhibits two

minima near each pore wall. These minima increase in magnitude and coalesce into one minimum for smaller pore diameters. The repulsive parts overlap for pore to particle size ratios near 1 and the potential depth decreases rapidly. In contrast to a flat surface, where the adsorbed particle interacts only with one or two surface atoms, a curved surface leads to an overlap of the van der Waals potentials. This overlap increases the adsorption strength for the particle even more for smaller pore diameters. [28–31] Additionally, the surface of porous materials may be composed of different elements, which can add an energetic heterogeneity to the adsorption potential.

2.1.1 Dihydrogen complexes

Dihydrogen bond to metal cations form complexes M^+-H_2, which provide a bridge between physisorbed and chemisorbed, i.e. between bound and dissociated states of dihydrogen. H_2 is bond to the metal center, but the H-H bond is still present. This bonding mechanism has not been found until 1984. [32]

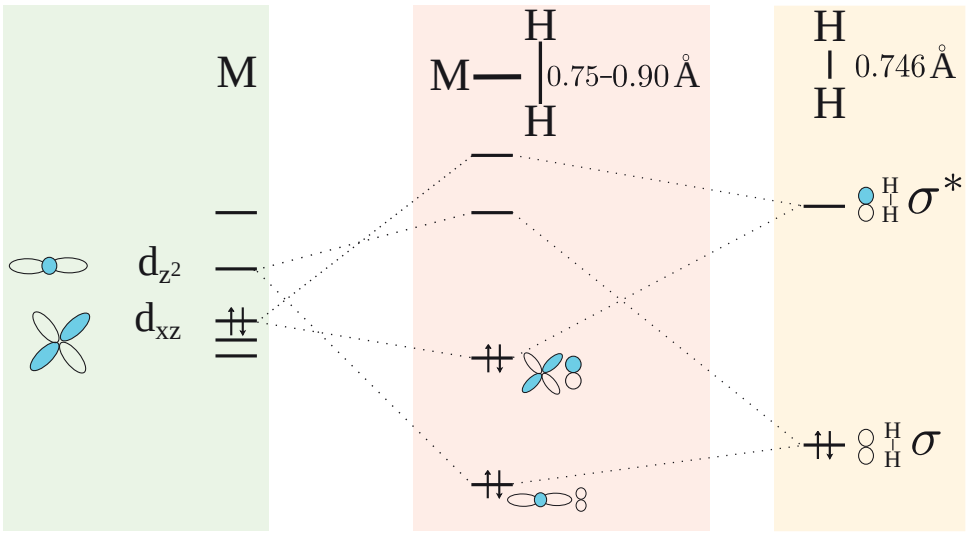

Figure 2.2: Illustration of the formation of dihydrogen complexes. The metal with its corresponding d orbitals is presented on the left side, the bonding (σ) and antibonding (σ^*) orbitals of hydrogen on the right side. In the middle the formation of the dihydrogen metal complex is shown. The bond length of the gaseous H_2 and the range for the elongation of the bond length due to the building of the complex are given above the energy levels. [33]

For building the M^+-H_2 complex, H_2 donates an electron from its σ bonding orbital into the d-orbitals of a metal and a back-donation from the metal occurs

in the empty σ^* antibonding orbital (figure 2.2). Intuitively, an antibonding orbital forming a chemical bond seems contradictory, but the σ^* orbital is only antibonding with respect to the bond between the H atoms and can still be bonding for the metal dihydrogen complex. The electron in the σ^* antibonding orbital and the half filled σ bonding orbital lead to a weakening of the H-H bond. Therefore, the bond length increases from 0.746 Å of a gaseous H_2 to values typically in the range of 0.75 Å-0.90 Å [34]. This increase in bond length comes with a decrease in vibrational frequency from 4160 cm^{-1} to a range between 2600-3000 cm^{-1} [35].

2.2 Isotope separation methods

2.2.1 Current methods for industrial separation of hydrogen isotopes and extraction of helium-3

Due to their identical chemical properties, hydrogen isotopes can only be separated by methods which use their different mass. The standard method for the enrichment of heavy water is the bithermal Girdler-sulfide process.

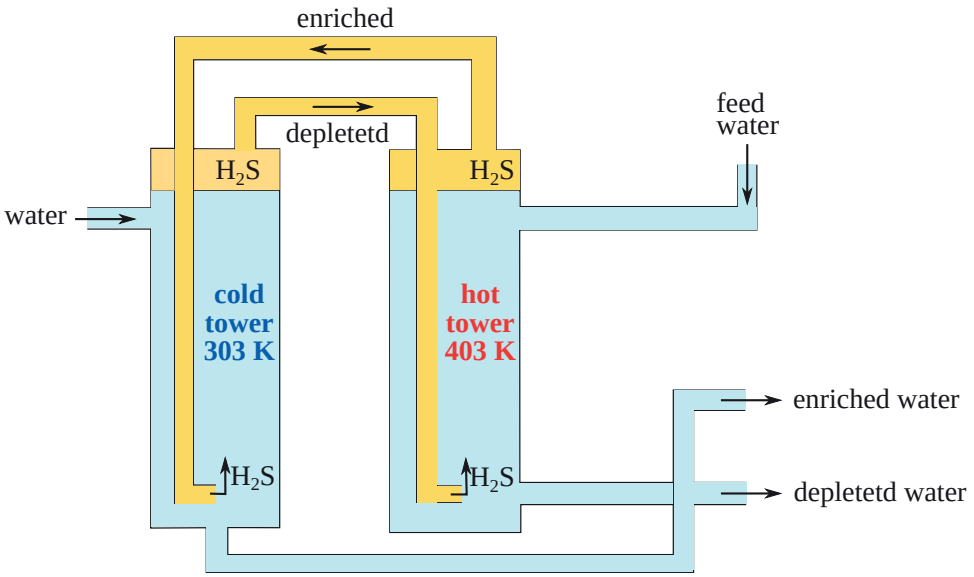

$$H_2O(l) + HDS(g) \rightleftharpoons HDO(l) + H_2S(g)$$

Figure 2.3: Concept of the Girdler-sulfide process for the production of heavy water.

This process uses the different equilibria of the reaction presented in figure 2.3 at 303 K and 403 K. [36] Hydrogen sulfide circulates as a gas in a closed loop between a cold tower and a hot tower, both filled with water. In the cold tower deuterium atoms migrate preferentially from the hydrogen sulfide gas to the liquid water. Fresh normal water with the natural abundance of deuterium is filled to the hot tower. There, the deuterium migrates from the water to the hydrogen sulfide gas, thereby enriching this gas. This enriched gas then again flows through the cold tower and further enrichment of the water takes place. The water leaving the hot tower has a lower concentration of deuterium atoms compared to when it entered the system. Multiple processing cycles lead to enriched water with 20%-30% [36] deuterium content. Further increasing of the purification is done with a vacuum distillation system, leading to a purity of approximately 99.75% of deuterium. The overall separation factor of this process is only 2.3 [9].
Another widespread technique for the purification of gases is the cryogenic distillation. The gases are cooled until they are liquefied and afterwards the components are selectively distilled at their individual boiling temperatures. Cooling to the low boiling points of hydrogen isotopes (20 K and 24 K [37] for H_2 and D_2, respectively) requires high energy consumption for the cooling process and their small temperature difference leads to low separation factor of 1.5 at 24 K [9].
Helium-3 is usually extracted as a byproduct of the radioactive tritium decay from tritium reserves of the nuclear weapons programs in the U.S. and Russia. [38] The reduction of the nuclear weapons stockpile and the increased demand for several applications resulted in a shortage of helium-3. This isotope also occurs in the atmosphere or in some natural gas sources. Therefore, direct extraction is also an option but was not used extensively in the past, as the supply with helium-3 was greater than the demand. [39]

2.2.2 Isotope separation with Quantum Sieving

In 1995 Beenakker *et al.* developed the theory of Quantum Sieving while investigating the adsorption of hard sphere molecules in cylindrical pores. When the difference between pore diameter d and hard core diameter σ of the molecule, becomes comparable to the de Broglie wavelength of the molecule [10]

$$\lambda_{deBroglie} \approx d - \sigma \tag{2.3}$$

a quantum mechanical treatment is required. This quantum mechanical treatment is particularly necessary at low temperature, where the de Broglie wavelength is larger. The model has been developed under the assumption of no molecule-molecule interaction and no molecule-surface interaction stronger than the van der Waals type. Therefore, the motion of the molecules in the pores is separated into the independent axial and radial ones. The axial motion is free between two consecutive collisions with phonons or surface defects, but the radial direction is restricted by a potential well created by the interaction with the pore walls. This potential has been approximated by a circular square well with the depth ϵ with respect to zero potential energy for a molecule in free space (see figure 2.4 left).

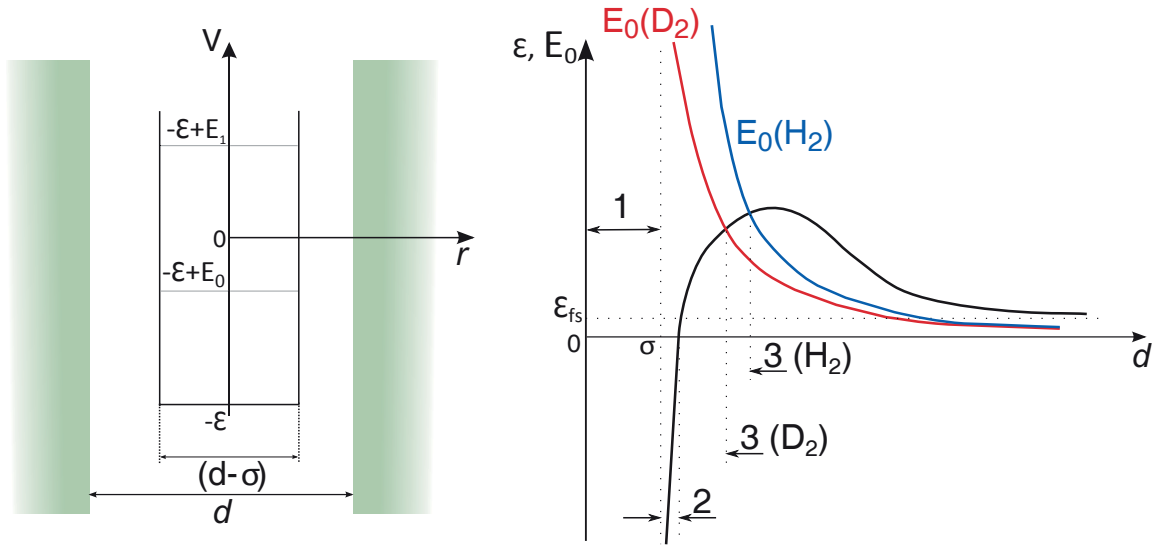

Figure 2.4: Left: Representation of the potential energy, V, for a molecule confined in a pore with $d - \sigma \approx \lambda$ and the transverse motion energy levels E_i. Right: The potential well depth ϵ and the zero-point energies of the isotopes in dependence on the pore diameter.

The energy levels E_i for a circular square well are [40]:

$$E_i = \frac{2\gamma_i^2 \hbar^2}{(d-\sigma)^2 m}, \tag{2.4}$$

where γ_i are related to the zeros of the Bessel functions. The potential well depth ϵ which represents the attraction of the walls and the zero-point energies are illustrated in figure 2.4 right as functions of the pore diameter. No adsorption is possible in region 1 because the hard core diameter exceeds the pore diameter. In region 2, where the pore gets slightly bigger than the hard core diameter, penetration is still difficult because the zero-point motion overcompensates the attraction of the molecule by the pore surface. Thus, the molecules encounter an energy barrier and the process of entering into the channel requires thermal excitation. In case of large pores the interaction potential is not affected by the opposite wall or curvatures and ϵ is simply the flat surface potential. The adsorption of a system is characterized by the relation of the zero-point energy and the potential well depth. The potential well is attractive for the molecule as long as the attraction of the walls overcompensates the zero-point energy of the molecule ($\epsilon > \mathrm{E}_0$). Figure 2.4 right depicts the different zero-point energies for hydrogen and deuterium according to their different masses. Hydrogen and deuterium have a mass ratio of 1:2, which is the largest value known for any two isotopes. With decreasing pore diameter hydrogen reaches earlier (at bigger diameters) the point marked with number 3, where it becomes more difficult to enter the pore compared to deuterium. The region where the zero-point energy of hydrogen already exceeded the attraction of the walls and penetration of deuterium is still possible represents the Quantum Sieving domain. As a consequence, in small pores and at temperatures below 100 K deuterium diffuses into the material faster than the lighter hydrogen. [41]

2.2.3 Isotope separation with Chemical Affinity Sieving

Chemical Affinity Sieving is a general concept for gas separation and the most commonly observed phenomenon in molecular sieving. [42] Molecules, which have the strongest chemical affinity with the pores are predominantly adsorbed by the pores.
A hydrogen molecule in the gas-phase has six degrees of freedom, namely three translational, two rotational and one vibrational, which contribute to the zero-point energy. If the adsorption potential is high, a barrier for diffusion on

the surface exists and the molecule looses the translational degrees of freedom parallel to the surface. The translational motion of the adsorbing molecule towards the surface can be thought of as the vibration of the species against the surface, i.e., to a vibrational motion in the potential energy well, which defines the adsorption itself. [43] Thus, the strength of an adsorption site has an impact on the zero-point energy of the adsorbed isotope. The different mass of isotopes leads to different zero-point energies for each isotope.

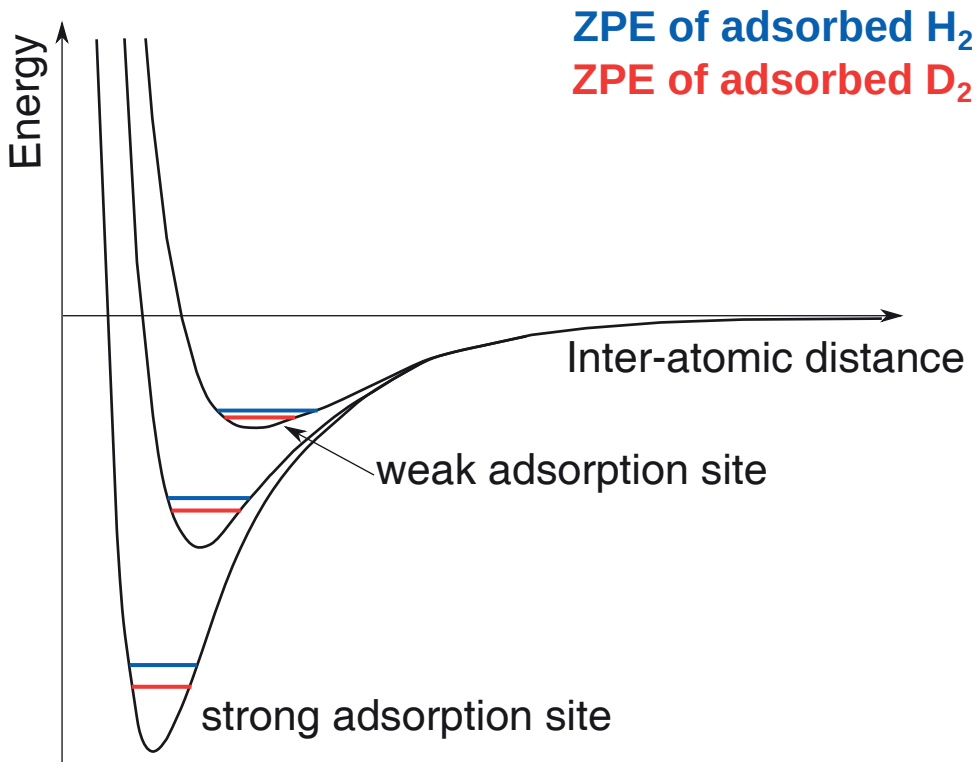

Figure 2.5: The different depths of the potential well represent the strength of the binding site. The zero-point energy of adsorbed hydrogen isotopes differ most on strong sites.

Figure 2.5 shows the impact of different adsorption strengths on the zero-point energy of hydrogen and deuterium. For a strong binding site the difference between the zero-point energies of the hydrogen isotopes is higher in comparison to a weak adsorption site, which results in a higher adsorption energy for the heavier isotope. Deep adsorption potentials lead to a high desorption temperature in the thermal desorption spectroscopy spectrum and the curvature of their potential well affects the selectivity. [44]

2.3 Thermal desorption spectroscopy

The thermal desorption spectroscopy (TDS) technique is a tool widely used in surface science and for the investigation of catalytic materials. [45–47] The experimental setup and procedure is described in chapter 3.1. For the TDS experiment a temperature program with a linear heating rate is applied to the material (adsorbent), which has been previously exposed to a gas at a given exposure temperature. During the temperature increase, the partial pressure of different gases is detected by a mass spectrometer in a continuously pumped system. These partial pressures are plotted versus the measured temperatures, resulting in a TDS spectrum. Considering a pumping rate high enough to prevent re-adsorption, each partial pressure is proportional to the desorption rate of the corresponding gas and the area under the full spectrum is proportional to the total amount of gas, which has been initially adsorbed at the exposure temperature. A TDS spectrum consisting of multiple desorption maxima implies that the material has several adsorption sites with distinct binding strengths. Respecting the principle of microscopic reversibility the adsorption and desorption process can be specified by the same set of rate equations. For one desorption maximum, the desorption rate r_{des} is described by a rate equation of n^{th} order:

$$r_{des} = -\frac{d\Theta}{dt} = k_n \cdot \Theta^n \tag{2.5}$$

where Θ is the instantaneous coverage and k_n is the rate constant, which gives the probability that a physisorbed gas molecule could escape back to the gas phase. The rate constant can be described by the *Arrhenius* equation:

$$k_n = \nu_n \cdot exp\left(\frac{-E_{des}}{RT}\right) \tag{2.6}$$

with ν_n as frequency factor, E_{des} is the desorption energy, R the gas constant and T the temperature. Combining eq. 2.6 and eq. 2.5 leads to the *Polanyi-Wigner* equation [48]:

$$r_{des} = -\frac{d\Theta}{dt} = \nu_n \cdot exp\left(\frac{-E_{des}}{RT}\right) \cdot \Theta^n \tag{2.7}$$

Combining this equation with the linear heating rate, β, and an initial temperature, T_0,:

$$T = T_0 + \beta t \tag{2.8}$$

yields:

$$-\frac{d\Theta}{dT} = \frac{\nu_n}{\beta} \cdot exp\left(\frac{-E_{des}}{RT}\right) \cdot \Theta^n \tag{2.9}$$

Figure 2.6 depicts the combination of the fractional coverage $\Theta(T)$ and the rate constant $k_n(T)$ to the TDS spectrum.

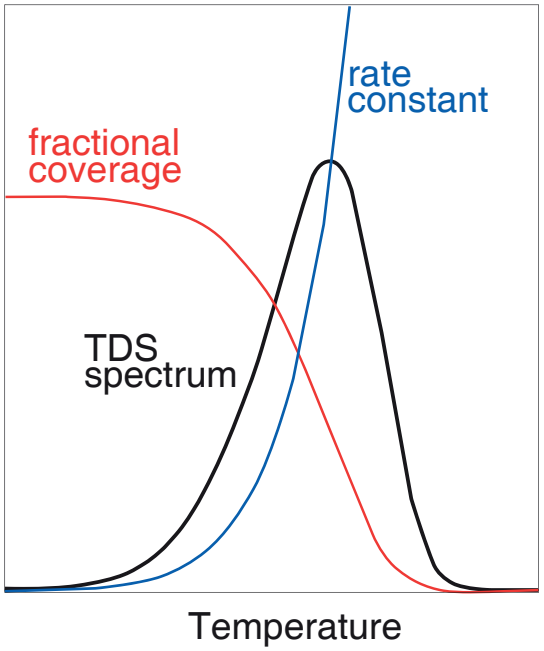

Figure 2.6: The measured desorption rate (TDS spectrum) is composed of the temperature dependent coverage and the rate constant.

Measuring the desorption for different initial coverages allows to determine the reaction order by the concentration dependence of the maximum temperature. Figure 2.7 depicts TDS spectra of different desorption orders n with different initial coverages.

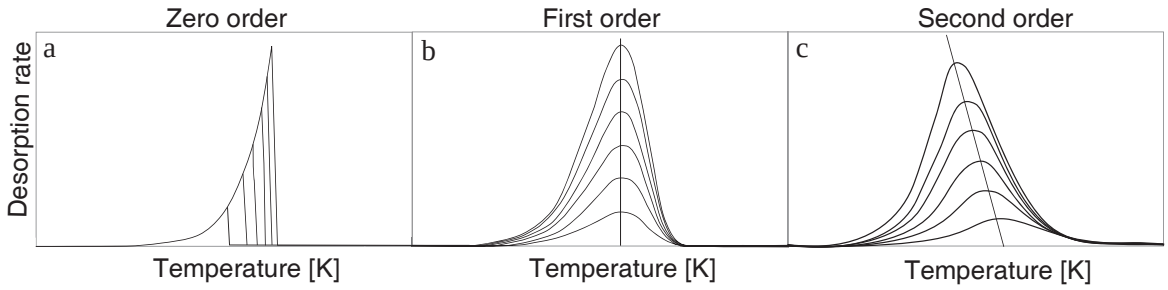

Figure 2.7: TDS spectra of different desorption orders. For higher coverages, the maximum temperature of the desorption rate shifts to (a) higher temperatures for zero-order desorption, (b) has no shift for first-order desorption and (c) shifts to lower temperatures for second-order desorption.

- Zero-order desorption process ($n = 0$) is described by the equation:

$$-\frac{d\Theta}{dT} = \frac{\nu}{\beta} \cdot exp\left(\frac{-E_{des}}{RT}\right) \tag{2.10}$$

  In this equation the desorption rate does not depend on coverage ($\Theta(T)$) and it increases exponentially with temperature until a rapid drop occurs when all molecules have been desorbed. The temperature of the peak maximum moves to higher temperatures with higher initial coverages (Θ_0). Zero-order kinetics is common if the adsorbate forms multilayers.

- First-order desorption process ($n = 1$) is described by the equation:

$$-\frac{d\Theta}{dT} = \frac{\nu}{\beta} \cdot exp\left(\frac{-E_{des}}{RT}\right) \cdot \Theta \tag{2.11}$$

  In case of first-order desorption the desorption rate is proportional to the fractional coverage ($\Theta(T)$). The temperature of the maximum is independent of the initial coverages. This desorption order represents the case of non-dissociative molecular and atomic adsorption.

- Second-order desorption process ($n = 2$) is described by the equation:

$$-\frac{d\Theta}{dT} = \frac{\nu}{\beta} \cdot exp\left(\frac{-E_{des}}{RT}\right) \cdot \Theta^2 \tag{2.12}$$

  The desorption rate of the second-order process is proportional to the square of the fractional coverage. The maximum temperature of the peak moves to lower temperature with increasing initial coverage. This desorption order is observed if re-combinative desorption occurs.